

EMERGENCE OF THE SVD AS AN INTERPRETABLE FACTORIZATION IN DEEP LEARNING FOR INVERSE PROBLEMS

SHASHANK SULE, RICHARD G. SPENCER, AND WOJCIECH CZAJA

ABSTRACT. Within the framework of deep learning we demonstrate the emergence of the singular value decomposition (SVD) of the weight matrix as a tool for interpretation of neural networks (NN) when combined with the descrambling transformation—a recently-developed technique for addressing interpretability in noisy parameter estimation neural networks [1]. By considering the averaging effect of the data passed to the descrambling minimization problem, we show that descrambling transformations—in the large data limit—can be expressed in terms of the SVD of the NN weights and the input autocorrelation matrix. Using this fact, we show that within the class of noisy parameter estimation problems the SVD may be the structure through which trained networks encode a signal model. We substantiate our theoretical findings with empirical evidence from both linear and non-linear signal models. Our results also illuminate the connections between a mathematical theory of semantic development [2] and neural network interpretability.

Interpreting the nature of the mapping between inputs and outputs of trained neural networks (NNs) remains one of the major unsolved problems in machine learning and is the focus of significant research effort [3, 4, 5, 6, 7, 8, 9, 10]. More recently, such efforts have succeeded in interpreting NN’s in image classification by examining the singular value decompositions (SVDs) of trained weight matrices [1, 11, 12, 13]. The SVD has innumerable applications in statistics [14, 15], dimensionality-reduction [16, 17, 18], and geometric data science [19, 20]. It has also found applications in specific deep learning settings, including sensing neural network topology [21], isotropic pattern recognition in control charts [22], and neural network weight compression [23]. The key idea behind using SVD for NN interpretation is that the singular subspaces of NN-associated matrices (such as weight matrices) adapt during training to encode learning. This is particularly natural when interpretation relies upon recognition of readily-identifiable patterns, such as image labels. Consequently, the hidden semantics of a trained NN may be uncovered by taking the SVD as a starting point and then applying a (possibly complicated) interpretation strategy such as intertwiner groups [12] or hypergraph rearrangements [13] of these SVDs. In this sense, an SVD-based interpretation strategy is a data-dependent processing of the SVD weights of the network which reveals a human-readable function implemented in each layer.

In this paper we show that this link between singular spaces and NN interpretation is more fundamental: the singular value decomposition itself emerges as an interpretation strategy. We specifically exhibit this phenomenon for *descrambling transformations* for interpretations of NNs used in optimization problems arising in signal processing [1]. Neural networks are now routinely used in various areas of science [24, 25, 26, 27] where network outputs are no longer simple class labels but are objects in a desired function space, and the network is trained to learn the underlying mapping between the input and output. While these networks often exceed the prior state-of-the-art methods in performance, their interpretability remains

an open question, as there usually is no relation of the network’s architecture to the physics of the problem at hand. To that end, we have focused on the SVD and the latent orthogonal transformations learned by the networks, motivated by the observation that many well-known transformations, such as e.g., the Fourier transform, are unitary and thus serve as a standard for human readability. This approach is quite promising: an analysis of linear two-layer neural networks [2] showed that the trained weight matrices exhibit specific relationships with the SVD of the covariance matrices from the distributions of the training data. In particular, if the network structure is given by $f(x) = W_2 W_1 x$, then the weights W_1 and W_2 in the large data limit obey the continuous-time evolution law (as the step size in gradient descent tends to zero) during training at time t :

$$(1) \quad W_2(t) = U A(\Lambda, t) Q^{-1}, \quad W_1(t) = Q A(\Lambda, t) V^\top.$$

Here U and V are the right and left singular vectors of the input-output correlation matrix $\Sigma_{yx} = \mathbb{E}[yx^\top] = U \Lambda V^\top$, and $A(\Lambda, t)$ is a diagonal matrix-valued function depending on the singular values Λ and the training time t . While this simple model shows that the singular vectors closest to input and output data learn semantics from the data distribution, an understanding of the intermediate weight matrices (matrices of the type Q in Equation 1) and the cases of nonlinear and deep networks remain unresolved. A major step in addressing this problem was taken in [1], in the context of digital signal processing, where the hidden layer semantics of DEERNet (a network used to solve a noisy Fredholm equation arising in electron-electron resonance) [28] were interpreted in [1] through the introduction of descrambling transformations.

The basic idea of descrambling is that a raw trained weight matrix W is uninterpretable or *scrambled*. Then a descrambling transformation given by multiplication by a particular matrix P —known as the *descrambler*—makes the corresponding matrix PW more interpretable to a subject matter expert. In this case, we can say PW is the “descrambled” form of W (see Figure 1). The descrambler P is selected as the *linear* transformation of the NN’s intermediate output that optimizes a user-selected criterion. Common choices of such criteria include smoothness, sparsity, or group invariance. Smoothness descrambling—descrambling to make the output of each layer maximally smooth—enabled the discovery of a notch filter and Chebyshev basis projection in the aforementioned DEERNet, leading to a “reverse-engineering” of the neural network where it was replaced by a deterministic transformation for processing DEER data.

Summary of results. Prompted by the pioneering empirical results in [1], the goal of our paper is to analyse the theoretical properties of smoothness criterion descramblers, with a focus on the case in which the network is trained to solve a noisy parameter estimation problem. We address the large data limits of the matrices as the number of training points in (2) tends to infinity. Our main finding is that the SVD naturally emerges as a large data limit of these descrambling transformations: Theorem 1 shows that when the first layer of the network is descrambled and the data is noise only, the limiting descrambler matrix can be written in terms of a trigonometric basis and the left singular vectors of the weight matrix W . We generalize this result to characterize the more realistic situation where the data $x = s(z) + \sigma\xi$ is obtained as noisy measurements of the signal z ; in this case we show that the descrambler *promotes* sinusoidality of the corresponding input/output signal library of the descrambled weight matrix and that the signal-to-noise ratio σ^{-1} parameterizes a continuous path from the large data limit descrambler $\widehat{\mathcal{P}}(1, X)$ to the identity matrix I .

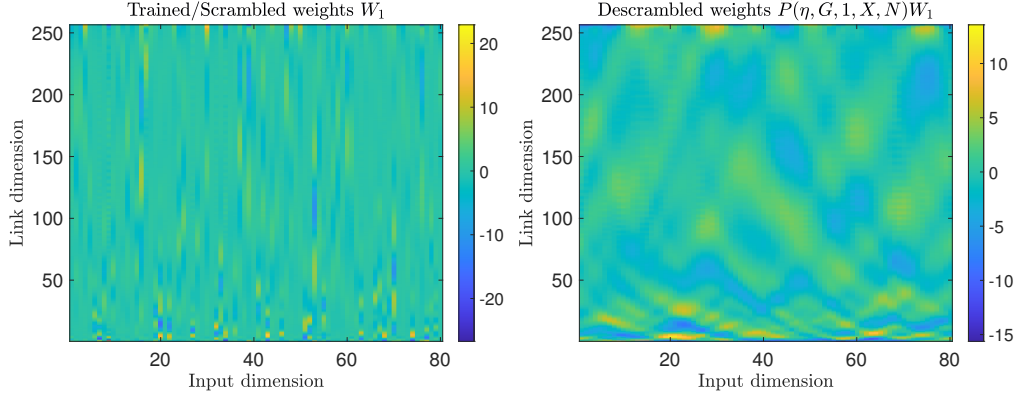


FIGURE 1. Left: Weight matrix W_1 of a trained shallow DEERNet with tanh activation. Right: Descrambled weight matrix $\hat{P}(\eta, G, 1, X, N)W_1$ where η is chosen to maximize smoothness of the output of the first layer and $G = O(m_1)$, the orthogonal group in m_1 dimensions, where m_1 is the width of the hidden layer. We see that descrambling the first weight matrix of DEERNet reveals interlocking wave-like patterns. In [1] these patterns are interpreted to be the time-domain representation of a notch filter, which informs the development of a first-principles based algorithm for processing DEER data. These interlocking patterns were not apparent in the original weight matrix W_1 , which appears to be nearly featureless and hence scrambled. In this way, multiplication by $\hat{P}(1, X, N)$ has “descrambled” W_1 and brought it into a more human-intelligible format.

We also show that in the case when the network is non-linear, the descrambler is related to the SVD of its *Jacobian* at the empirical mean of the data (Figure 3). In this way we show that the choice of the data model plays a crucial role not only in training but also in interpretation via descrambling. In particular, we show how the signal-to-noise ratio in the training data, which is independent of the NN, affects the descrambler matrix $\hat{P}(k, X, N)$ (Theorem 2).

While the mathematical aspects of our main results are interesting in their own right and will be discussed in the following sections, we highlight here three important consequences of our results. First, we observe that our results on the sinusoidality of descrambled weights give a theoretical account of the empirical results obtained for the descrambling analysis of DEERNet [1]. As a consequence we can provide a quantitative justification for the fact that Fourier domain visualization yields intelligible representations of descrambled weights. Second, we show how descrambling can define classes of problem-dependent *interpretable* networks—networks where descramblers converge to the identity transformation—and how convolutional neural networks emerge as interpretable networks for certain inverse problems. Third, we find that descrambling networks by providing purely noisy data *still* allows for an interpretation of the weights, leading us to conjecture that the forward map is memorized [29] in the right singular vectors of the first weight matrix, without necessarily memorizing instances of training data. We confirm this conjecture empirically in two different examples of noisy signal recovery—DEER spectroscopy and biexponential parameter estimation—noting that right singular vectors of the first weight matrix closely resemble the training data model.

Neural Network Descrambling. In neural network descrambling we interrogate, or *wiretap*, the network’s output F at the k th layer with a matrix P (2) in the following sense: P is computed as the minimizer of a well-chosen objective function η over a specified group G :

$$(2) \quad F = \sigma W_L \cdots \sigma P^{-1} P \overbrace{W_k \cdots W_1}^{f_k(X)} X$$

$$(3) \quad \hat{P}(\eta, G, k, X, N) = \underset{P \in G}{\operatorname{argmin}} \eta(P f_k(X)).$$

Here X denotes the matrix of the training data, which we assume is drawn from a context-dependent prior distribution. It has N columns, where each column is an input vector. The motivation for choosing P to range over the representation of a group G is that any matrix P that successfully wiretaps a neural network represents an interpretable rearrangement of the nodes, and the composition of any two rearrangements should also be a rearrangement. This assumption leads naturally to a group structure on the search space of the minimization problem.

In the framework of NN descrambling, the raw weights W_k obtained after training are considered *scrambled* and the weights after multiplication by the descrambler $\hat{P}(\eta, G, k, X, N)$ are termed *descrambled*. Thus, the descramblers defined in Equation 3 seek to transform the outermost weight matrices W_k into interpretable objects in the context of the training data. In this paper, we mathematically analyse a particular class of descramblers, namely the *smoothness descramblers* used in [1] for NN interpretation. Smoothness descrambling is the specialization of (3) in which the minimizers $\hat{P}(\eta, G, k, X, N)$ —henceforth termed descramblers—are computed to promote smoothness of the intermediate data, i.e., the output of each layer, over the orthogonal group $G = O(n)$. The motivation behind this choice of NN interpretation is that while the network’s incoming and outgoing data is usually smooth and has an intelligible time-ordered structure, the intermediate data often loses this structure. As such, the role of the descrambler is to change basis so that the intermediate signal is itself smooth and thus ordered with respect to the indices of the output or input dimension. Thus, the objective function η_{SC} used for maximizing the smoothness of the intermediate data is given as follows:

$$(4) \quad \eta_{SC}(P f_k(X)) = \|DPW_k \circ \sigma \circ \cdots W_1 X\|_F^2.$$

The descramblers \hat{P}_{SC} are obtained as the minimizers of η_{SC} over the orthogonal matrices $O(n_k)$, where n_k is the number of neurons in the k th layer:

$$(5) \quad \hat{P}_{SC}(k, X, N) := \hat{P}(\eta_{SC}, O(n_k), k, X, N) := \underset{P \in O(n_k)}{\operatorname{argmin}} \|DP f_k(X)\|_F^2 \quad \text{w.r.t } P^\top P = I.$$

It is difficult to say anything specific about the structure of the general $\hat{P}_{SC}(k, X, N)$, as in principle it can be used for any model of any problem. In consequence we focus on the case where X models data used in inverse problems, as in the initial demonstration of the descrambling transformations. Thus, each column of X can be written as a noisy measurement $s(z) + \sigma\xi$ where z is a to-be-recovered vector, ξ is (white) noise, and σ^{-1} is the SNR. We will first describe the case when the network is linear and the input is only noise and then generalize to the case where the output has an underlying signal. Finally we will treat the case when the network is non-linear. All proofs have been outlined in the Supplementary Information.

RESULTS

We proceed to characterize the minimizers of (5)—the smoothness criterion descrambling problem. We will describe the behaviour of \hat{P} for different layers k as the training set size $N \rightarrow \infty$. Our main mathematical innovations are (i) separating the cases $k = 1$ (when f_k is affine) and $k \geq 2$ and (ii) modeling X as sampled over a distribution given by the noisy measurement of a signal z with a known prior. We are primarily concerned with the role of the SNR σ^{-1} in affecting the descramblers \hat{P}_{SC} . This enables us to model the real-life settings in which neural networks used for inverse problems are trained and evaluated. We state our main theoretical results below.

Linear Network, Only Noise. We first address the case when $k = 1$ in (5). In this case, $f_1(x) = W_1x$, so the wiretapped network f_1 is linear. We first consider the case where X is pure noise, i.e $x_i \sim \xi$ where ξ is a zero mean isotropic random variable. The canonical example is the standard normal variable $\xi \sim N(0, I)$ where the covariance matrix is given by the identity matrix I of the relevant dimension. Our strategy to understand the minimizers of (5) is to study the convergence of $\hat{P}_{SC}(1, X, N)$ as $N \rightarrow \infty$. We shall see that these descramblers $\hat{P}_{SC}(1, X, N)$ have a limit $\hat{P}_{SC}(1, x)$ given by the (strong) law of large numbers (SLLN). However, to use the SLLN to swap a limit and a minimum, we need to ensure the stability of the singular spaces of the random matrices WX . Bearing this in mind we first introduce the following technical definition.

Definition 1. Let $A_{n,m} \subseteq M_{n,m}(\mathbb{R})$ be the set of matrices with distinct non-zero singular values. Let $\mathcal{A} = \bigcup_{n,m} A_{n,m}$ be the set of *admissible matrices*. A fully-connected feedforward NN with weights $W_k \in \mathcal{A}$ is termed an *admissible neural network*.

Henceforth, we shall only work with admissible neural networks. In practice, this is not a restriction; since $A_{n,m}$ is a dense subset of $M_{n,m}$, admissible neural networks are dense in the set of all NNs. The definition of admissibility allows us to ensure the stability of singular subspaces under limits. This is the consequence of the continuity of the simple eigenvalues of a matrix in its entries [30, Theorem 6, Chapter 9]:

Lemma 1. Let A_n be a sequence of square matrices such that $A_n \rightarrow A$ in the Frobenius norm, where $A \in \mathcal{A}$. Then, the left and right singular vectors $\{a_i^n\}$ and $\{b_i^n\}$ of A_n converge to the left and right singular vectors of A , respectively.

Note that for $k = 1$, we can simplify (5). In particular, since the data matrix X has N columns we denote $X_N := X$ and set $k = 1$ in (5) to get

$$(6) \quad \hat{P}_{SC}(1, X, N) = \operatorname{argmin} \|DPW_1X_N\|_F^2 \quad \text{w.r.t } P^\top P = I.$$

First, we note that W_1 has dimensions $m_1 \times d$. Next, we make the following assumptions modelling the empirical setup in [1]:

- (1) D is a Fourier differentiation matrix or a finite difference matrix [31].
- (2) X is a random $d \times N$ matrix such that each column X_i is drawn independently from a zero-mean isotropic distribution x .
- (3) T is the $m_1 \times m_1$ matrix such that every k th column has l th entry $t_k(l)$ given by

$$(7) \quad t_k(l) = \begin{cases} \cos \frac{\pi l k}{m_1} & k \text{ even} \\ \sin \frac{\pi l (k+1)}{m_1} & k \text{ odd.} \end{cases}$$

With these assumptions we can show that as the number of samples N tends to infinity, $\hat{P}_{SC}(1, X, N)$ can be expressed in terms of the matrix T and the SVD of W_1 .

Theorem 1. Let f be an admissible NN with W_1 as its first layer weight matrix with rank- r SVD $W_1 = {}^rU_1 {}^r\Sigma_1 {}^rV_1^\top$, where ${}^rU_1, {}^r\Sigma_1, {}^rV_1$ denote the components of the economic, rank- r SVD. Additionally, let T_r be the matrix formed by selecting the first r columns of T . Then,

$$(8) \quad \hat{P}_{SC}(1, X, N) \longrightarrow \hat{P}(1, x) := T_r {}^rU_1^\top \text{ almost surely with } N \rightarrow \infty.$$

In particular, the descrambled weight matrix converges to $T_r {}^r\Sigma_1 {}^rV_1^\top$ almost surely in the measure induced by x .

Thus, under certain geometric assumptions for the data X (isotropic, zero mean, finite second moment), trained weight matrices descrambled for smooth propagation of data exhibit a sinusoidal basis. This choice of X corresponds to the noise model in many signal processing applications. We illustrate this effect in Figure 2 where we visualize the left singular vectors of a descrambled weight matrix for the first layer of a fully connected neural network from [32]. We also note that Theorem 1 produces a scaling law $P \rightarrow T_r^\top P {}^rU_1$. Under this scaling law, the descramblers $\hat{P}_{SC}(1, X, N) = T_r {}^rU_1^\top$ converge to identity I as $N \rightarrow \infty$. We will use this scaling law to justify the use of Fourier domain visualizations in [1]. We provide a more general version of Theorem 1 in the supplementary information; here the choice of D as a Fourier difference stencil was taken to align the result with the experimental setup used in [1]

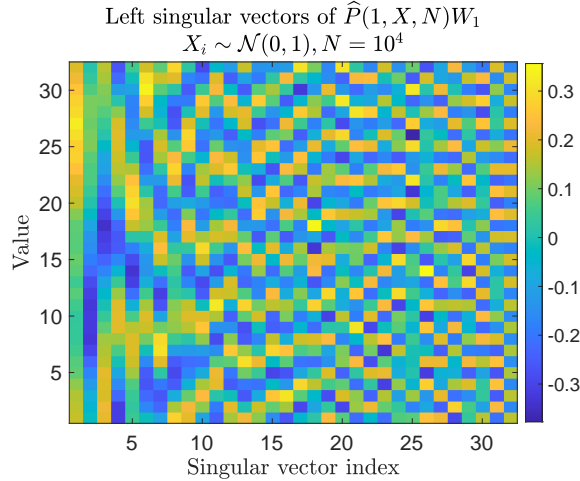


FIGURE 2. We sampled X in Equation 5 from a standard Gaussian ensemble and computed the left singular vectors of the first layer pre- and post-descrambling of the network in [32]. Note that the left singular vectors of the descrambled weight matrix are perfectly oscillating: this is because X as a standard Gaussian ensemble together with a linear wiretapped layer yields a descrambler $\hat{P}(N) \approx T_r U^\top$, which results in $\hat{P}W \approx T_r \Sigma V^\top$ so that the left singular vectors of the descrambled weight matrix are given by T_r

Linear Network, Noise and Signal. In more realistic applied settings, training data is usually a mixture of signal and noise; we extend Theorem 1 to this case below. For this we consider the case when each training sample is $x = s(z) + \sigma\xi$.

Theorem 2. With the notation from Theorem 1, let $X_N(\sigma)$ be a $d \times N$ matrix of training data where each column is sampled from $x(\sigma) = s(z) + \sigma\xi$. Denote

$$\widehat{\mathcal{P}}_{SC}(1, x(\sigma)) := \lim_{N \rightarrow \infty} \widehat{\mathcal{P}}_{SC}(1, X_N(\sigma), N)$$

and let $\widehat{\mathcal{U}}_1(\sigma)$ be the matrix of left singular vectors of the descrambled weight matrix $\widehat{\mathcal{P}}_{SC}(1, x(\sigma))W_1$. Then $\widehat{\mathcal{U}}_1(\sigma)$ is continuous in σ and as $\sigma^{-1} \rightarrow 0$

$$(9) \quad \|\widehat{\mathcal{U}}_1(\sigma) - T_r\|_F = O(\sigma^{-2}) \rightarrow 0.$$

Theorem 2 shows that the left singular vector basis of the descrambled matrix is “close” to a trigonometric basis, to an extent controlled by the SNR σ^{-1} . As $\sigma^{-1} \rightarrow 0$ this basis converges to the trigonometric basis (which is consistent with the case of Theorem 1).

Non-linear network. Finally, we discuss the non-linear case when $k \geq 2$. In this situation we choose to analyze non-linearities by applying the previous results to the first-order Taylor expansion at the sample mean \bar{X} :

$$(10) \quad \widehat{\mathcal{P}}_{SC}(1, X_N(\sigma), N) \approx \underset{P^\top P = I}{\operatorname{argmin}} \mathbb{E}[\|DP(f_k(\bar{X}) + Jf_k(\bar{X})(X - \bar{X}))\|_2^2].$$

The RHS can be characterized through Theorems 1 and 2 applied to $Jf(\bar{X})$. We provide empirical evidence for the quality of the Jacobian approximation to the descrambling problem in Figure 3.

Applications.

Interpretable neural networks. We use the results presented in the preceding discussion to study two cases in which we can confirm that descrambling reveals information that can be validated through other well-understood transformation of the weights. The first example comes from convolutional neural networks (CNNs). As a preliminary remark, we note that CNNs can be understood as fully connected NNs by setting the appropriate weights to zero, and thus can be brought under our framework for studying descramblers for fully connected NNs.

Corollary 1. Adopting the assumptions of Theorem 1 with samples of noise X and $k = 1$, let f be a 1-D CNN with stride 1. Then $\widehat{\mathcal{P}}_{SC}(1, X)W_1 = W_1$, i.e., descrambling acts as the identity transformation on the weight matrix.

Corollary 1 presents a simple case where the descrambled weight matrix is itself, so that interpretability is not enhanced by descrambling. This indicates that every choice of η , G , and X from (3) defines a class of *interpretable* neural networks $\mathcal{I}(\eta, G, k, X)$ such that the descramblers $\widehat{\mathcal{P}}_{SC}(\eta, G, k, X, N)$ converge to the identity I in the large data limit whenever $f \in \mathcal{I}(\eta, G, k, X)$. We formalize this intuition below. In what follows we assume that \mathcal{N} is the set of fully connected neural networks.

Definition 2. An interpretability class $\mathcal{I}(\eta, G, k, x \sim \mu) \subset \mathcal{N}$ is the set of neural networks such that $f \in \mathcal{I}(\eta, G, k, x \sim \mu)$ if, for the k th layer, a group G , criterion η , and data X the solution to (3) where X has N i.i.d. columns sampled from μ is $\widehat{\mathcal{P}}(\eta, G, k, x \sim \mu) = I$ as $N \rightarrow \infty$. If $f \in \mathcal{I}(\eta, G, k, x)$ then f is said to be $\mathcal{I}(\eta, G, k, x)$ -interpretable, or simply \mathcal{I} interpretable when η, G, k and x are clear from context.

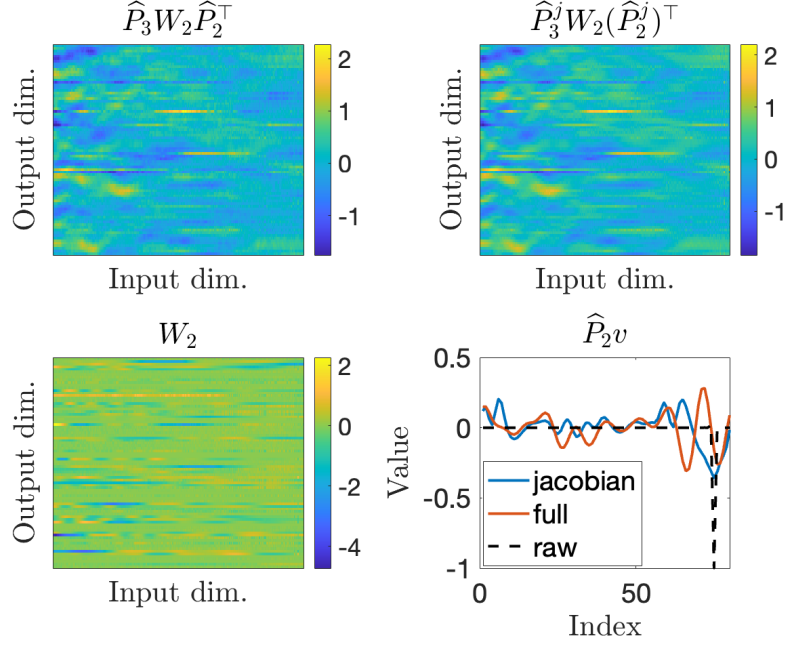


FIGURE 3. We compare the descramblers computed for $k = 2$ in DEERnet with $f_2(X)$ (denoted as full) and with the approximation in (10) (denoted as Jacobian). We find that the overall descrambled matrices are visually similar (albeit of limited interpretability). We also see, via the illustrated action of \hat{P} on the 64th singular vector (denoted as raw), that the Jacobian descramblers \hat{P}^j are an intermediate between full descrambling and no descrambling (bottom right). Note that the raw singular vector is especially sparse, taking only one non-zero value at the 78th index. We attribute this sparsity to the use of ReLU activations used in our implementation of a shallow DEERnet. The relative mean absolute errors (RMAE) for \hat{P}_2^j vs \hat{P}_2^j and \hat{P}_3^j vs \hat{P}_3^j were 1.25% and 0.4% respectively.

Interpretability classes define NNs which cannot be further interpreted by descrambling, given the choices of η, G , and X . These \mathcal{I} -classes are defined in terms of the underlying problem (such as signal recovery or image classification) by tracking the distribution on the training data. Furthermore, Definition 2 models a simple but natural setting used for training various types of neural networks: the training inputs are an incoming stream of samples of x forming the matrix of samples X . Under this training data regime, \mathcal{I} -interpretability records the large-data behaviour of the descrambler \hat{P} for a specific choice of wiretapped layer and descrambling criterion. *A priori* interpretability classes have a rather complicated structure and it is a mathematically interesting problem to provide some better understanding of different cases. In fact, we can reformulate Corollary 1 to give an explicit presentation for $\mathcal{I}(\eta_{SC}, O(n), 1, x \sim N(0, \sigma^2 I))$ as the class of neural networks which contain 1-D convolutions in the first layer.

Corollary 2. Let $k = 1$, $G = O(n)$, η_{SC} be the smoothness criterion (5) and let x be distributed with a zero-mean isotropic random-variable. Let $\mathcal{C}_1^n \subset \mathcal{N}$ with a convolutional first layer with n nodes in the first hidden layer and let \mathcal{N} be the class of $1 - D$ NNs in

$C(\mathbb{R}^n)^m$. Then, we have

$$(11) \quad \mathcal{I}(\eta_{SC}, O(n), 1, x \sim N(0, \sigma^2 I)) = \mathcal{C}_1^n.$$

As such, characterizing $\mathcal{I}(\eta_{SC}, O(n), 1, (x, N(0, \sigma^2 I)))$ may seem unrealistic because most real-life instances of neural network training do not utilize purely noisy data. However, recalling the context of inverse problems, it is of interest to know whether we can characterize any interpretability class when the input data is in the form of noisy measurements of a parameter. It turns out, for instance, that a simple phase identification problem in oscillatory data analysis (ODA) can be the right setting for such a question. A central problem in ODA is to identify the phases $\phi(t)$ and the trend $T(t)$ from the measurements of the noisy signal

$$(12) \quad f(t) = \exp 2\pi i \phi(t) + T(t) + y.$$

The signal model in (12) is ubiquitous in many applications of science and engineering, including clinical, seismic, and climate data, and investigative art [33, 34, 35, 36, 37, 38, 39, 40]. Unsurprisingly, this type of inverse problem has attracted neural network approaches [41]. Here we show that in the simple case when the trend $T = 0$ and the phase $\phi(t) = \alpha t$, where α is a constant to be estimated under a uniform prior, the oscillatory data modeled by (12) defines a setting where we can characterize an interpretability class.

Corollary 3. Let $\alpha \sim \text{Unif}[-uM, vM]$ be the phase parameter with uniform prior for $u, v \in \mathbb{Z}$ and the oscillating signal $s(z) = (\exp 2\pi i k \alpha / M)_{k=0}^{M-1}$ be measured as $x = s(\alpha) + \sigma \xi$ where ξ is a standard normal variable. Then

$$(13) \quad \mathcal{I}(\eta_{SC}, O(n), 1, x) = \mathcal{C}_1^n.$$

Here \mathcal{C}_1^n is the class of neural networks with a convolutional first layer and n nodes in the first hidden layer.

Corollary 3 has multiple implications. For example, it shows that CNNs reside in the class of interpretable networks for the problem of recovering the phase from equispaced samples of a signal oscillating time. Second, it shows that the first layer of a network trained to solve this inverse problem cannot be further interpreted by descrambling, because the descrambler transformation converges to the identity matrix; smoothness descrambling reveals to us only the information already available in the raw weights of the first layer.

DEERNet. We use our theoretical analysis to furnish quantitative justifications for the previously-reported pioneering visual descrambling analysis of DEERNet [1], the neural network on which descrambling was first tested. This theoretical perspective will illuminate how the SVD emerges as an “interpretable” factorization. DEERNet is a feedforward neural net trained to solve an inverse signal estimation problem in double electron-electron resonance spectroscopy. In particular, it solves the following Fredholm equation of the first kind:

$$(14) \quad \Gamma(t) = \int_{\Omega} p(r) \gamma(r, t) dr + \sigma \xi.$$

Here ξ is considered to be white noise and $\gamma(r, t)$ is the DEER kernel given by

$$(15) \quad \gamma(r, t) := \sqrt{\frac{\pi}{6Dt}} \left[\cos[Dt] C \left[\sqrt{\frac{6Dt}{\pi}} \right] + \sin[Dt] S \left[\sqrt{\frac{6Dt}{\pi}} \right] \right]$$

$$(16) \quad D := \frac{\mu_0}{4\pi} \frac{\gamma_1 \gamma_2 h}{r^3}; \quad C(x) = \int_0^x \cos(t^2) dt; \quad S(x) = \int_0^x \sin(t^2) dt.$$

In the above equation, γ_1, γ_2 are gyromagnetic ratios. In DEERNet, the training inputs and outputs to the network are of the form $\{\Gamma_i, p_i\}_{i=1}^N$, where p_i are distributions and Γ_i are the measurements detected at times $\{t_j\}_{j=1}^{256}$ according to (15). DEERNet obtains p_i from Γ_i and hence can be formulated as a network that solves the problem of recovering z from noisy observations of $x = s(z) + \sigma\xi$. Here s represents the integral operator in the DEER kernel (15) and z is the input probability distribution.

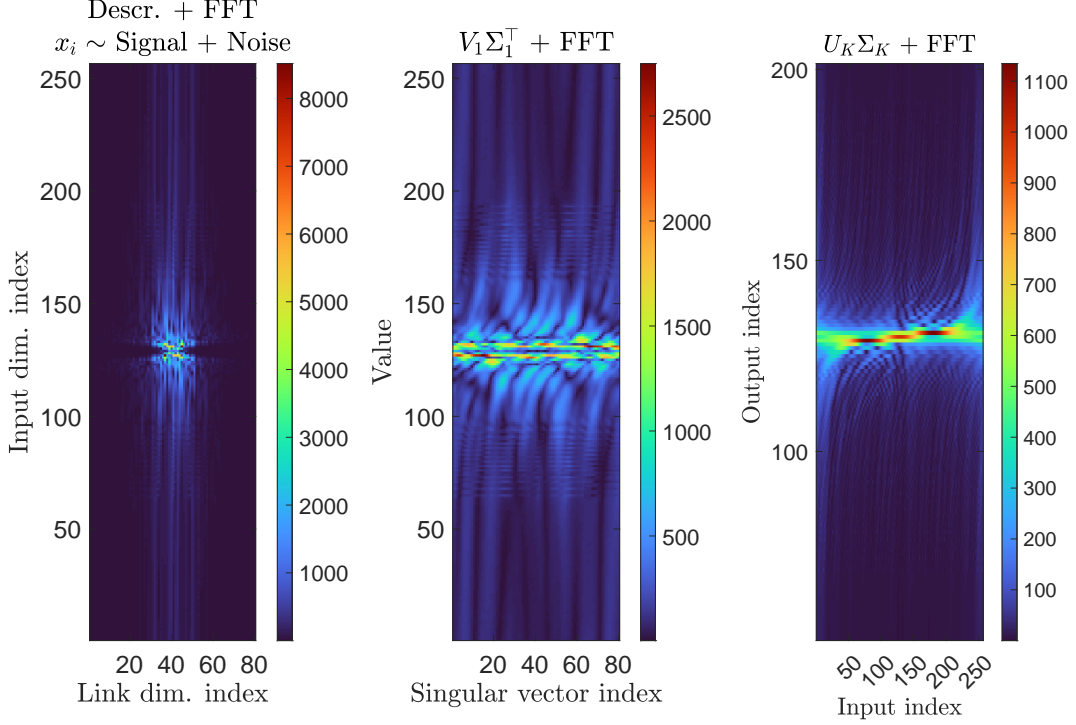


FIGURE 4. Left: Descrambling the first layer of a two-layer DEERNet reveals a notch and bandpass filter. A powerful plausibility argument is mounted in [1] to indicate that this notch resembles a cube on the time axis/input dimension appearing in the DEER kernel (15). Center: Visualization of the Fourier transform of $\Sigma_1 V_1^T$ reveals repeating patterns along the singular vectors; in fact, along the time axis we see these patterns roughly corresponding the shape of a cubic. Right: We visualize the Fourier transform of the right singular vectors of the integral kernel K scaled by the singular values Σ_K and observe cubic streaks similar to those in the central panel. This provides a more quantitative justification for the first layer’s function as inverting the integral operator.

Why Fourier domain visualization works. Here we fix $\eta = \eta_{SC}$ and $G = O(n)$, denoting descramblers as $\hat{P}_{SC}(k, X, N)$. In [1] a descrambling analysis of the first layer weights of a shallow 2-layer DEERnet uncovered a notch filter and a bandpass filter in the first weight matrix after visualizing the 2-D DFT of $\hat{P}_{SC}(1, X, N)W_1$ (Figure 4). This Fourier domain visualization was justified experimentally because of the interlocking wave patterns seen in the descrambled weights $\hat{P}_{SC}(1, X, N)W_1$ in Figure 1. We now provide a more quantitative justification for this heuristic, based on Theorem 1 and on the correspondence

between the SNR σ^{-1} and the descrambling matrix $\hat{P}_{SC}(1, X, N)$. Our justification is as follows: when the descrambling data X is spherical or pure noise, $\hat{P}_{SC}(1, X, N)$ converges to $T_r r U_1^\top$ due to Theorem 1. As a consequence, $T_r^\top \hat{P}_{SC}(1, X, N) r U_1$ converges to the identity matrix I . Thus, the group homomorphism

$$(17) \quad P \rightarrow \varphi(P) = T_r^\top \hat{P}(1, X, N) r U_1$$

provides an appropriate rescaling for the limiting descrambling matrix $\hat{\mathcal{P}}(1, x)$. For example, when σ^{-1} converges to 0, $\varphi(\hat{\mathcal{P}}_{SC}(1, x(\sigma)))$ converges to I almost surely. Thus the group homomorphism (17) simplifies the correspondence between the SNR and the rescaled large-limit descrambler $\varphi(\hat{\mathcal{P}}_{SC}(1, x))$. Under this correspondence we have:

$$(18) \quad \text{SNR} = 0 \longleftrightarrow \varphi(\hat{\mathcal{P}}_{SC}(1, x)) = I.$$

As a consequence the 2D DFT of descrambled W_1 given by $\mathcal{F}\hat{P}(1, X, N)W_1\mathcal{F}^\top$ approximates

$$(19) \quad \varphi(\hat{\mathcal{P}}_{SC}(1, x)) r \Sigma_1 (\mathcal{F}^\top V_1)^\top.$$

In fact, in the case when $\varphi(\hat{\mathcal{P}}_{SC}(1, x)) = I$, $\mathcal{F}\hat{P}_{SC}(1, X, N)W_1 \approx r \Sigma_1 (\mathcal{F}^\top V_1)^\top$ —the Fourier transform of the singular vectors rescaled by the singular values. Thus, visualizing the matrix by setting $\varphi(P) = I$ is quite informative: the result approximates $r \Sigma_1 (\mathcal{F}^\top V_1)^\top$ and it reveals a repeating pattern of cubic streaks, uncovering both the notch filter and the distance cube root as found in the integral kernel from (14), as pointed out in [1]. This shows that descrambling uncovers—to a large extent—the information within the SVD and that multiplication by $\hat{P}_{SC}(1, X, N)$ moves W_1 closer to the integral kernel. Singular vectors themselves are interpretable without necessitating any additional processing such as descrambling, intertwiner groups, or hypergraph arrangements [13, 12] in the context of noisy signal estimation.

Connection to semantic development. The emergence of the DEER kernel in the right singular vector matrix V_1 can be predicted from the exact solutions to neural network training dynamics given in (1). Indeed, if the network f did not have a non-linearity, then f would be a *deep linear network* (DLN). DLNs are simplified models of neural networks used for studying the convergence and generalization properties of NNs; in fact it was pointed out in [2] that the training dynamics of deep neural networks are approximated by those of DLNs. Assuming now that DEERnet is a DLN given by $f(x) = W_2 W_1 x$, then as the step-size of gradient descent tends to zero, f trained on RMSE observes the following time-evolution law,

$$(20) \quad W_1(t) = Q^{-1} A(\Lambda, t) V^\top,$$

where V is the matrix of the right singular vectors of $\Sigma_{yx} = \mathbb{E}[yx^\top]$, the output-input covariance matrix. Although the formula 20 depends on the input-input correlation matrix Σ_{xx} to equal the identity I , it was shown in [42] that 20 holds under the weaker assumption where

$$(21) \quad \Sigma_{yx} = U S V^\top,$$

$$(22) \quad \Sigma_{xx} = V \Lambda V^\top.$$

Here U, V are orthogonal matrices and S, Λ are diagonal matrices. Interestingly, the data used for inverse problems with linear forward maps (such as inputs and outputs for DEER-Net) satisfies this weaker assumption. In particular, let the forward map be given by $s(z) = Kz$. Furthermore, let the training inputs, the noisy observations, be given by $x = Kz + \sigma\xi$ and the training outputs by $y = z$. Supposing (without loss of generality) that $\mathbb{E}[z] = 0$, we have

$$(23) \quad \Sigma_{yx} = \mathbb{E}[zz^\top]K^\top := \Sigma K^\top,$$

$$(24) \quad \Sigma_{xx} = K\mathbb{E}[zz^\top]K^\top := K\Sigma K^\top + \sigma I.$$

Here we used the independence of the prior distribution z and the isotropicity of the noise distribution ξ . Now, since Σ is symmetric positive semidefinite (as it is a covariance matrix of the random variable z), we may write we write the SVD $K\sqrt{\Sigma} = V S U^\top$. Introducing this formula into the above equations yields

$$(25) \quad \Sigma_{yx} = \Sigma U S V^\top := U' S' V^\top,$$

$$(26) \quad \Sigma_{xx} = V(S^2 + I)V^\top.$$

Thus, the input data satisfies Equation 22. Consequently, for the DLN approximation to the shallow DEERNet, Equation 20 holds for W_1 . Thus the right singular vectors of W_1 – V_1 –coincide with the with the left singular vectors of $K\sqrt{\Sigma}$ after training. Assuming that $\sqrt{\Sigma} \approx dI$, i.e that the covariance matrix of the prior distribution is approximately diagonal, we should obtain that the Fourier transform of the descrambled weights is approximated by the spectral decomposition of the discretized DEER kernel K . Remarkably, this approximation turns out to be qualitatively accurate—we illustrate this fact in Figure 4.

Descrambling with sphered data. Our analysis of DEERnet shows that descrambling reveals semantic development during training in the singular vectors of NN weights, particularly when a network is trained to learn a signal from noisy measurements. However, this interplay with semantic development is an approximation. This is because the linear network training dynamics (1) can only approximate the real training dynamics of nonlinear networks. Furthermore, achieving the specific diagonalization of the correlation matrices Σ_{yx}, Σ_{xx} in (22) is possible only when the forward map is linear or if the input data is isotropic, i.e it is whitened or *sphered*. Sphered data arises widely in several deep learning contexts including batch normalization [43], convergence analyses of NN training [44], and image data preprocessing [45].

Theorem 1 indicates that descrambling with sphered data converts the weight matrix into the Fourier transform of the right singular vectors. Here we show a case where such an interpretation, i.e the inspection of singular vectors, is useful in and of itself. We demonstrate this case for a NN in which the forward map s is non-linear, so that the nature of matrices U and V in (1) is entirely unspecified. In particular, following [32], we train a four layer fully-connected NN to learn the exponential parameters $(T_{2,1}, T_{2,2})$ generating a biexponential model corrupted by noise:

$$(27) \quad y(t) = c_1 \exp(-t/T_{2,1}) + c_2 \exp(-t/T_{2,2}) + \sigma\xi.$$

The recovery of exponential parameters $T_{2,1}, T_{2,2}$ from a noisy decay curve is a central problem in magnetic resonance (MR) relaxometry [46] and it arises as follows. After excitation by a radio-frequency pulse, the net magnetization of excited nuclei (typically the proton nuclei of the hydrogen atoms in water) relaxes, or decays, in the plane transverse to the main magnetic

field of the MR system. The time constant of this decay, denoted T_2 , depends upon the chemical environment of the relaxing nuclei; for example, more motionally-restricted nuclei relax more rapidly, exhibiting a smaller T_2 value. Therefore, when this proton spin relaxation occurs simultaneously in chemically distinct environments characterized e.g. by different water mobilities, the signal will consist of two or more components corresponding to these environments. In the important case in which the relaxing system can be modeled by two dominant components [47, 48, 49, 50, 51], we recover the biexponential signal (27), where $T_{2,1}$ and $T_{2,2}$ are the respective decay time constants of the component fractions described by the corresponding factors multiplying the exponential terms. This system is known to be ill-posed [52] with parameter estimates strongly dependent upon the noise component of the signal. This problem has been investigated with a number of neural network-based approaches [53, 54]; the novelty of the network in [32] is that it is trained to solve this problem on both noisy and smooth forms of the same data, as a form of input data transformation to incorporate high-fidelity, high-stability, and generalizability characteristics into the solutions. To achieve this, the noisy input data is first processed with regularized non-linear least squares parameter estimation, with these estimates used to generate smooth decay curves. These smooth curves are concatenated with the noisy samples to form a single input sample for presentation to the NN. The NN with just the native input, concatenated with itself, is termed (ND, ND), where ND indicates noisy decay. The NN with the concatenated native and smoothed versions of the decay curve is termed (ND, Reg), with Reg indicating the smooth decay generated by the regularized nonlinear least squares analysis. This strategy of training on both noisy and smooth data is termed *input layer regularization*, and improves parameter estimation by 5-10 percent as compared to the more conventional NN estimation of parameters from noisy decay curves [32]. In Figure 5, we show that the right singular vectors corresponding to the largest singular values of the first layer are biexponential curves, so that the network learns an input signal library in the class of its training data. Most notably, the (ND, Reg) network learns two very different shapes of biexponential for the noisy and smooth case; we attribute its higher test accuracy as compared to (ND, ND) to this result, indicating that (ND, Reg) learns a larger set of functions within the signal model class of biexponential functions. Thus, in the regression setting the descrambling guides us to finding the location of NN learning, namely within the SVD. In addition to explaining generalization, learning of the model in the SVD may have implications for data privacy since we are able to learn samples of the input data model directly from a trained network. While the SVD has been used as a compression technique in feedforward neural networks [23] and deep layer interpretation in classification [11, 13], our results appear to be the first demonstration that data model learning occurs in singular vectors for nonlinear deep networks.

DISCUSSION

A key novelty of descrambling is that it exploits problem-dependent interpretation, akin to the manner in which interpretability methods in image classification center upon the most influential pixels, image substructures, and decision boundaries. We take this concept further: our characterization of solutions to (5) and the subsequent theoretical framework for the experimental results in [1] show that the interpretation matrices \hat{P} can admit simple large-data limits that depend on the underlying problem. In fact, we observe that the mathematical formalism of inverse problems allows us to obtain strong characterizations of these

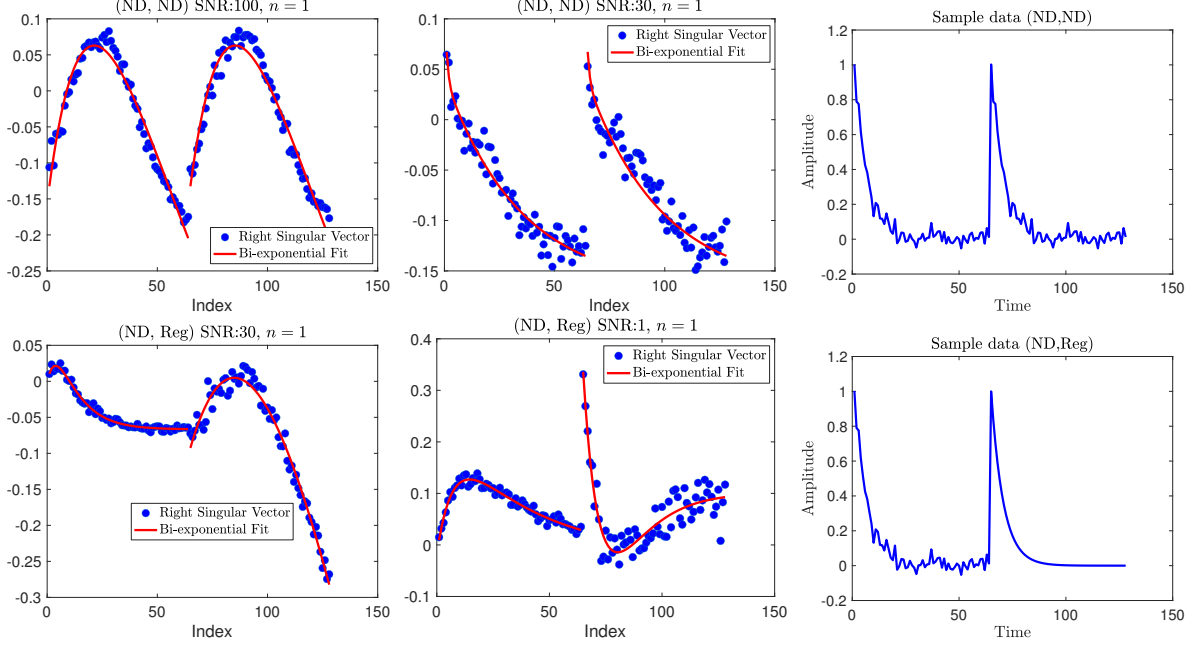


FIGURE 5. We visualize the singular vectors of the first layer of ILR networks trained on concatenations of noisy time-series data with the functional form $c_1 \exp(-t/T_{2,1}) + c_2 \exp(-t/T_{2,2})$ for $c_1 = 0.6, c_2 = 0.4$. Top row, left and center: The top singular vectors of the (ND, ND) networks for the first layer, for $\sigma^{-1} = 1, 100$. Top row, right: A sample training point in the (ND, ND) network. Bottom row: Same analysis as top row, for (ND, ND) networks, for $\sigma^{-1} = 1, 30$. Bottom row, right: A sample training point for the (ND, Reg) network. Note that the second half of the signal is a smooth version of the noisy first half. We find that the dominant singular vectors of the first layer weights themselves can be fit by curves of the same algebraic form as the noiseless version of the training data, allowing for the c_i 's to be negative. However, while the (ND, ND) networks learn the same biexponentials in each halves of the singular vectors, each right singular vector of the weights of the (ND, Reg) networks learn exhibits markedly different biexponentials in either half. This phenomenon occurs across a wide range of SNR's and for both classes of networks—(ND, ND) and (ND, Reg). Here (ND, Reg) refers to networks trained on data points given by a concatenation of noisy and Tikhonov regularized copies of the same data, while (ND, ND) refers to networks trained on concatenation of the noisy data to itself.

limits with practical implications. For example, descrambling implicitly defines problem-dependent classes of neural networks - and these classes can be explicitly characterized, for instance, in a simple problem from oscillatory data analysis. Furthermore, while [1] provides an interpretation of DEERNet through the SVD of the descrambled weights, we show that even the SVDs of the *scrambled*, i.e., raw, weights can themselves be informative. We have given an explanation for this phenomenon in Section 2; if the data is highly corrupted by noise, the Fourier domain visualization of the descrambled weights approximates the Fourier

domain visualization of the orthogonal row basis vectors provided by the right singular vectors through the rescaling formula motivated by Theorem 1. We remark, however, that this does not imply that descrambling is equivalent to the SVD; indeed, in the cases when the data X follows the more realistic distribution of a noise corrupted signal and the network is wiretapped at a higher layer ($k \geq 2$) we can no longer exactly characterize the solutions to (5) and the minimizers do indeed reflect the latent transformations in the underlying weights W_k . We find empirically that the action of descrambler matrices can be approximated through descrambling of the network linearized by its Jacobian evaluated at the empirical average of the data. This does not mean the choice of the Jacobian as a linear approximation is canonical—there are many different linear models for NN’s [55, 56, 57] and it is yet unclear which approximation serves best as a surrogate for modeling the action of descrambling transformations.

A surprising and significant aspect of our results is that when the SVD is uncovered indirectly by descrambling, it *still* remains informative of the transformations in the data. This observation closely resembles examples [13, 12, 58] where SVDs of weights in CNNs are used to interpret features of an image classification network. Unlike these approaches, which require highly non-trivial post-processing of the singular vectors, we demonstrate that a simple visual analysis of singular vectors themselves may be able to inform the post hoc analysis of the trained network’s performance. Moreover we show that in noisy estimation problems it is the SVD where the network memorizes the underlying function class of the problem. This demonstrates not only that the training dynamics given by (1) for linear models can approximate non-linear settings but also that the SVD by itself can illuminate the network’s generalizability and interpretability.

MATERIALS AND METHODS

DEERNet. In Figures 1, 3, and 4, we descrambled DEERNet according to the specifications in [1]. The training inputs $\{p_i\}$ were synthetically generated to match multimodal DEER distributions [28]. The training outputs were then given by $\Gamma_i = Kp_i + \sigma\xi$, where K is a matrix discretization of the integral operator in Equation 15, ξ is white noise, and σ^{-1} is the SNR, chosen here to be 10. Each input-output pair thus corresponds to (p_i, Γ_i) . DEERnet was then defined with the architecture Input \rightarrow Fully connected $256 \times 80 \rightarrow$ tanh activation \rightarrow Fully connected $80 \times 256 \rightarrow$ sigmoid activation \rightarrow renormalization \rightarrow Output. Additionally, we made use of the MATLAB modules in the Spinach package to train the network and descramble it on a Quadro GV100 GPU to reproduce the experiments in [1] as closely as possible. We have given a quantitative explanation for why the first layer represents the DEER kernel based on a rescaling analysis motivated by our Theorem 1. We also confirmed the notion put forward by Amey et al. of the appearance of the cubic functional form based in the appearance of cubic power in the kernel (14) by changing this power to a quartic, and finding a narrowing in the notch. This is consistent with the fact that a quartic curve is flatter around the origin than a cubic. This experiment has been provided in our data repository <https://github.com/ShashankSule/descrambling-NN>.

ILR network. We trained two neural networks—termed *conventional* and *ILR*—with a $128 \rightarrow 32 \rightarrow 256 \rightarrow 256 \rightarrow 2$ architecture with ReLU non-linearities to solve the problem of recovering $(T_{2,1}, T_{2,2})$ from noisy measurements of the signal y in Equation (27). We synthetically generated these noisy measurements for $T_{2,1}$ and $T_{2,2}$ each ranging uniformly in the interval $[50, 500]$, for 64 equispaced times in the interval $[0.0, 800.0]$. The resulting noisy vector is

termed ND. The conventional and ILR networks differed only in terms of the postprocessing of this noisy vector into generation of training input. For the conventional network, the noisy vector was concatenated with itself to form the input vector (ND, ND); the network was then trained to recover the combination of $(T_{2,1}, T_{2,2})$ used for generating the noisy vector ND. For the ILR network, however, ND was processed through a non-linear least squares (NLLS) algorithm with Tikhonov regularization, and the resulting NLLS-recovered parameters $(T_{2,1}^{NLLS}, T_{2,2}^{NLLS})$ were used to generate a new noiseless signal termed Reg, for "regularized". The ILR network was then trained to recover the $(T_{2,1}, T_{2,2})$ combination used for generating ND from concatenated pair (ND, Reg). Both NNs were trained using a RMSE loss function. For regularization we followed [32] and used a Tikhonov regularization procedure in the NLLS pre-processing step with $\lambda = 1.6 \times 10^{-4}$. After training, we computed the singular vectors of the weight matrices W_1 , finding that these singular vectors themselves are noisy samples of biexponential curves, although unlike the training data, for which we required $c_1, c_2 \geq 0$ for physical reasons, the SV's of the trained weight matrix could correspond to positive or negative values for these coefficients. We infer from this that the first layer learns the general signal model rather than training examples themselves, or, equivalently, that imposed constraints are not incorporated in a simple fashion. We have presented more comprehensive data evaluating over the three leading singular vectors for both conventional and ILR networks in the SI document for SNR values $\sigma^{-1} = 1, 30, 100$.

Proofs and code availability. All our theoretical results have been proven in the SI document. Code for the figures and additional experiments can be found at <https://github.com/ShashankSule/descrambling-NN>

ACKNOWLEDGEMENTS

This work was supported in part by the Intramural Research Program of the National Institute on Aging of the National Institutes of Health (NIH).

APPENDIX

THEORETICAL RESULTS

Here we provide proofs for the results in the main text. For readers' convenience, we repeat the statements of the results.

Lemma 1. Let A_n be a sequence of matrices such that $A_n \rightarrow A$ in the Frobenius norm, where $A \in \mathcal{A}$. Then, the left and right singular vectors $\{a_i^n\}$ and $\{b_i^n\}$ of A_n converge to the left and right singular vectors of A , respectively.

Proof. Since a_i^n and b_i^n are the eigenvectors of $A_n A_n^\top$ and $A_n^\top A_n$ respectively, we consider, without loss of generality, the case of symmetric W , and accordingly of real eigenvalues. From [30, Theorem 8, pp. 130], the eigenvectors of a matrix with simple eigenvalues are differentiable with respect to its entries. Consequently, if a_i^n is the i th eigenvector of A_n then $a_i^n \rightarrow a_i$ where a_i is the i th eigenvector of A . The same applies to b_i^n . \square

Theorem 1. We make the following assumptions:

- (1) D is a Fourier differentiation matrix.
- (2) X is a random $d \times N$ matrix such that each column X_i is drawn independently from a zero-mean isotropic distribution x .
- (3) T is the $m_1 \times m_1$ matrix such that every k th column has l th entry $t_k(l)$ given by

$$(7) \quad t_k(l) = \begin{cases} \cos \frac{\pi l k}{m_1} & k \text{ even,} \\ \sin \frac{\pi l (k+1)}{m_1} & k \text{ odd.} \end{cases}$$

Let f be an admissible NN with W_1 as its first layer weight matrix with rank- r SVD $W_1 = {}^r U_1 {}^r \Sigma_1 {}^r V_1^\top$, where ${}^r U_1, {}^r \Sigma_1, {}^r V_1$ denote the components of the economic, rank- r SVD. Additionally, let T_r be the matrix formed by selecting the first r columns of T . Then,

$$(8) \quad \widehat{P}_{SC}(1, X, N) \longrightarrow \widehat{\mathcal{P}}(1, x) := T_r {}^r U_1^\top \text{ almost surely with } N \rightarrow \infty.$$

In particular, the descrambled weight matrix converges to $T_r {}^r \Sigma_1 {}^r V_1^\top$ almost surely in the measure induced by x .

Proof. We consider the more general case when D is any matrix with a rank- r singular value decomposition $D = R \Omega T^\top$. The statement of the theorem will follow from the fact that the matrix of samples of trigonometric functions (7) diagonalizes the symmetric and circulant Fourier differentiation stencil. For notational convenience, we set $X_N := X$ and let $S_N := \frac{1}{\sqrt{N}} W X_N$. Note that

$$\operatorname{argmin}_{P^\top P = I} \|DPW X_N\|_F^2 = \operatorname{argmin}_{P^\top P = I} \frac{1}{N} \|DPW X_N\|_F^2.$$

Then,

$$(28) \quad \frac{1}{N} \|DPW X_N\|_F^2 = \frac{1}{N} \text{Tr}(DPW X_N (DPW X_N)^\top)$$

$$(29) \quad = \frac{1}{N} \text{Tr}(DPW X_N X_N^\top W^\top P^\top D^\top)$$

$$(30) \quad = \text{Tr} \left(DPW \left(\frac{1}{N} X_N X_N^\top \right) W^\top P^\top D^\top \right)$$

$$(31) \quad = \text{Tr}(DPS_N S_N^\top P^\top D^\top)$$

$$(32) \quad = \text{Tr}(S_N^\top P^\top D^\top DPS_N).$$

To find the minimizer to (32) w.r.t $P^\top P = I$ we change variables: let $U_N \Sigma_N V_N$ be the SVD of S_N . Then we let $Y_N = P S_N V_N$. Note that this means $Y_N^\top Y = \Sigma_N^2$ given the constraint $P^\top P = I$. With this change of variables (32) can be written as

$$(33) \quad \frac{1}{N} \|DPW X_N\|_F^2 = \text{Tr}(Y^\top D^\top D Y).$$

Consequently, the smoothness descrambling problem

$$(34) \quad \min \|DPW X_N\|_F^2 \quad \text{w.r.t } P^\top P = I$$

can be relaxed to

$$(35) \quad \min \text{Tr}(Y^\top D^\top D Y) \quad \text{w.r.t } Y^\top Y = \Sigma_N^2.$$

Note that the optimization problem Eq. (34) is a relaxation of Eq. (35) because of the transformation $P \rightarrow P W V$. But now the solution to the relaxed problem (35) is well-known: it is a generalized eigenvalue problem whose solutions correspond to the first $R_N = \min(r_N, r)$ eigenvectors of $D^\top D$ where r_N is the number of non-zero diagonal entries in Σ_N^2 . Since $D^\top D$ is diagonalized by T , we pick the largest R_N eigenvectors (indexed by the matrix T_{R_N}) and scale them by Σ_N to get Y . Thus, $Y = T_{R_N} \Sigma_{R_N}$. Now using the change of variables $Y = P S_N V_{R_N}$ we get $P S_N = T_{R_N} \Sigma_{R_N} V_{R_N}^\top$ so $S_N = P^\top T_{R_N} \Sigma_{R_N} V_{R_N}^\top$. This is a singular value decomposition for S_N , so, provided the non-zero singular values of S_N are distinct, we obtain from the uniqueness of the SVD that $\hat{P}_N^\top T_{R_N} = U_N \iff \hat{P}_N = T_{R_N} (U_N)_{R_N}$. We now use the assumption that $W \in \mathcal{A}$: due to the strong law of large numbers we have that $S_N S_N^\top \rightarrow W W^\top$ almost surely. Since the singular values of $W W^\top$ are distinct, the singular values of $S_N S_N^\top$ are eventually distinct and ordered according to the order of $W W^\top$. This means that the singular values of S_N are distinct so the expression for $\hat{P}_N = T_{R_N} (U_N)_{R_N}$ is valid, where U_N are the singular vectors of S_N . But the columns of U_N are also the eigenvectors of $S_N S_N^\top$, which due to the law of large numbers, converges to $W_N W_N^\top$. But now U_N converges to U_1 due to Lemma 1 and this proves our result. \square

Theorem 2. With the notation from Theorem 1, let $X_N(\sigma)$ be a $d \times N$ matrix of training data where each column is sampled from $x(\sigma) = s(z) + \sigma \xi$. Denote

$$\hat{\mathcal{P}}_{SC}(1, x(\sigma)) := \lim_{N \rightarrow \infty} \hat{P}_{SC}(1, X_N(\sigma), N),$$

and let $\hat{\mathcal{U}}_1(\sigma)$ be the matrix of left singular vectors of the descrambled weight matrix $\hat{\mathcal{P}}_{SC}(1, x(\sigma)) W_1$. Then $\hat{\mathcal{U}}_1(\sigma)$ is continuous in σ and as $\sigma^{-1} \rightarrow 0$

$$(36) \quad \|\hat{\mathcal{U}}_1(\sigma) - T_r\|_F = O(\sigma^{-2}) \rightarrow 0.$$

Proof. Let $x(\sigma) = s(z) + \sigma\xi$ where ξ is a zero-mean isotropic noise vector with finite second moment and z has a bounded prior distribution independent of the noise y . We first observe the following law of large numbers (LLN) behavior:

$$(37) \quad \eta(P) \rightarrow \mathbb{E}[\|DPW_1(s(z))\|_2^2] + \sigma^2 \mathbb{E}[\|DPW_1\xi\|_2^2].$$

The proof of (37) is as follows: Note first that because of the LLN,

$$\frac{1}{N} \|DPW_1 X\|_F^2 = \frac{1}{N} \sum_{i=1}^N \|DPW_1 x_i\|_2^2 \rightarrow \mathbb{E}_{z,y}[\|DPW_1 x\|_2^2].$$

We directly switch to analyzing the LLN limit of η and write

$$\eta(P) = \mathbb{E}[\|DPW_1 x\|_2^2] = \mathbb{E}[\mathbb{E}[\|DPW_1 x\|_2^2 \mid z]] = \mathbb{E}[\mathbb{E}[\|DPW_1(s(z) + \sigma\xi)\|_2^2 \mid z]].$$

Now setting $A = DPW_1$ and using the assumed zero-mean property of the additive noise we get

$$\begin{aligned} \eta(P) &= \mathbb{E}\left[\mathbb{E}[\|A(s(z))\|_2^2 \mid z] + \mathbb{E}[\|A(\sigma\xi)\|_2^2 \mid z] \right. \\ &\quad \left. + 2\sigma\mathbb{E}[\langle A^\top A(s(z)), \xi \rangle \mid z] \right] \\ &= \mathbb{E}\left[\mathbb{E}[\|A(s(z))\|_2^2 \mid z] + \mathbb{E}[\|A(\sigma\xi)\|_2^2 \mid z] \right] \\ &= \mathbb{E}[\|A(s(z))\|_2^2] + \sigma^2 \mathbb{E}[\|A\xi\|_2^2] \\ (37) \quad &= \mathbb{E}[\|DPW_1(s(z))\|_2^2] + \sigma^2 \mathbb{E}[\|DPW_1\xi\|_2^2]. \end{aligned}$$

We can use the same analysis as the proof of Theorem 1 to conclude first that $\hat{P}_N = T_{R_M}(U_N)_{R_N}$; here U_N is the matrix of left singular vectors of $W_1 \frac{1}{N} (X_N X_N^\top) W_1^\top$. To analyse the limit as $\sigma^{-1} \rightarrow 0$, we first note that from the LLN and the zero mean property of ξ ,

$$(38) \quad W_1 \frac{1}{N} (X_N X_N^\top) W_1^\top \rightarrow \Sigma(\sigma) := W_1 (\mathbb{E}[s(z)s(z)^\top] + \sigma^2 I) W_1^\top$$

$$(39) \quad = \sigma^2 W_1 W_1^\top + W_1 \mathbb{E}[s(z)s(z)^\top] W_1^\top.$$

Due to eigenvector continuity, $U_N \rightarrow U(\sigma)$ where $U(\sigma)$ is the matrix of eigenvectors of $\Sigma(\sigma)$. We intend to measure the deviation of U_1 , the eigenvectors of $W_1 W_1^\top$ from $U(\sigma)$. Note that for every σ , the singular vectors of $\Sigma(\sigma)$ are identical to those of $\sigma^{-2}\Sigma(\sigma)$. But $\sigma^{-2}\Sigma(\sigma) = W_1 W_1^\top + \sigma^{-2}W_1 \mathbb{E}[s(z)s(z)^\top] W_1^\top$. Now, since $W_1 W_1^\top$ has distinct eigenvalues $s_1 \leq \dots \leq s_d$, we can set $C = \min\{|\lambda_i - \lambda_{i+1}|\}_{i=1}^d$. Furthermore, we may, without losing generality, consider the signs of the singular vectors $U(\sigma)$ to be such that $[U(\sigma)^\top U_1]_{ii} \geq 0$ for every $1 \leq i \leq d$. This allows us to use the modified Davis-Kahan theorem [59, Corollary 1] to show:

$$(40) \quad \|U_1 - U(\sigma)\| \leq \frac{2^{3/2} \|W_1 W_1^\top - \sigma^{-2}\Sigma(\sigma)\|}{C} = \frac{2^{3/2} \sigma^{-2}}{C} \|W_1 \mathbb{E}[s(z)s(z)^\top] W_1^\top\|.$$

Thus, as $\sigma^{-1} \rightarrow 0$, $U(\sigma)$ converges to U . Here $\|\cdot\|$ is the operator norm of the relevant matrix. \square

Finally, we state and prove Corollaries 1 and 2 pertaining to convolutional neural networks and oscillatory data analysis:

Corollary 1. Adopting the assumptions of Theorem 1 where data is sampled with a zero mean isotropic distribution and $k = 1$, let f be a 1-D CNN with stride 1. Then $\widehat{P}(1, X, N)W_1 = W_1$, i.e., descrambling acts as identity transformation on the weight matrix.

Proof. If f is a 1-D CNN where the first filter W has stride 1 then W is symmetric and circulant so $W = T\Sigma_1 T^\top$ where T is the matrix of samples of a trigonometric basis from Theorem 1. Then from Theorem 1, $\widehat{P}(1, X, N) = T_r^\top T_r = I_r$. \square

Corollary 1. Adopting the assumptions of Theorem 1 where data is sampled with a zero mean isotropic distribution and $k = 1$, let f be a 1-D CNN with stride 1. Then $\widehat{P}(1, X, N)W_1 = W_1$, i.e., descrambling acts as identity transformation on the weight matrix.

Proof. If f is a 1-D CNN where the first filter W has stride 1 then W is symmetric and circulant so $W = T\Sigma_1 T^\top$ where T is the matrix of samples of a trigonometric basis from Theorem 1. Then from Theorem 1, $\widehat{P}(1, X, N) = T_r^\top T_r = I_r$. \square

Corollary 2. Adopting the assumptions of Theorem 1, let $\alpha \sim \text{Unif}[-uM, vM]$ for $u, v \in \mathbb{Z}$ and $s(\alpha) = (\exp 2\pi i k \alpha / N)_{k=0}^{N-1}$. Then $\widehat{P}(N) \rightarrow \widehat{P} = T_r U^\top$ where T_r is the trigonometric basis from Theorem 1 and U is the left singular vector matrix of the weights W .

Proof. We show that the signal term and noise term reduce to the same minimization problem. Let $A := DPW$. Then we have

$$\mathbb{E}_\alpha[DPW s(\alpha)] = \mathbb{E}_\alpha[As(\alpha)] = \frac{1}{N(u+v)} \int_{-uN}^{vN} \|As(\alpha)\|_2^2 d\alpha.$$

But now, $(As(\alpha))_j \overline{(As(\alpha))_j} = \sum_{k,l} a_{jk} a_{jl} \exp 2\pi i(k-l)\alpha/N$, and

$$(1/N(u+v)) \int_{-uN}^{vN} \exp 2\pi i(k-l)\alpha/N d\alpha = \delta_{l,k}.$$

Here $\delta_{k,l}$ is the Kronecker delta. Now,

$$\begin{aligned} \frac{1}{N(u+v)} \int_{-uN}^{vN} \|As(\alpha)\|_2^2 d\alpha &= \frac{1}{N(u+v)} \int_{-uN}^{vN} \sum_j (As(\alpha))_j \overline{(As(\alpha))_j} d\alpha \\ &= \sum_j \frac{1}{N(u+v)} \int_{-uN}^{vN} (As(\alpha))_j \overline{(As(\alpha))_j} d\alpha \\ &= \sum_j \sum_k |a_{j,k}|^2 \\ &= \|A\|_F^2 = \|DPW\|_2^2. \end{aligned}$$

Putting the above calculation together with the calculation for isotropic noise from Theorem 1 and using Equation (37) we get

$$\begin{aligned} \eta(P) &= \mathbb{E}_\alpha[DPW s(\alpha)] + \sigma^2 \mathbb{E}[\|DPW \xi\|_2^2] \\ &= \|DPW\|_2^2 + \sigma^2 \|DPW\|_2^2. \end{aligned}$$

Minimizing the above function for P orthonormal leads to $P = T_r^\top U$ (as for Theorem 1). \square

MDS Criterion. The *maximum diagonal sum* (MDS) criterion is suggested in [1] for NN interpretation of frequency domain data:

$$\hat{P}_{MDS} = \operatorname{argmax}_{P^\top P = I} \operatorname{Tr}(PW)$$

We show that for this criterion \hat{P} can be given explicitly in terms of the SVD of weights W :

Proposition. Let $W \in M_n(\mathbb{R})$. Then $\operatorname{argmax}_{P^\top P = I} \operatorname{Tr}(PW) = VU^\top$ where $W = U\Sigma V^\top$ is the SVD of W .

Proof. Let $W = \sum_{i=1}^r \sigma_i u_i v_i^\top$ be the SVD of W and let P be orthogonal. Then,

$$\operatorname{Tr}(PW) = \sum_{i=1}^r \sigma_i \operatorname{Tr}(Pu_i v_i^\top).$$

But note that $\operatorname{Tr}(xy^\top) = \langle x, y \rangle$ so $\operatorname{Tr}(Pu_i v_i^\top) = \langle Pu, v \rangle \leq \|Pu\|^2 \|v\|^2 = 1$ using the Cauchy-Schwarz inequality. Therefore

$$\operatorname{Tr}(PW) = \sum_{i=1}^r \sigma_i \operatorname{Tr}(Pu_i v_i^\top) \leq \sum_{i=1}^r \sigma_i = \operatorname{Tr}(\sqrt{W^\top W}).$$

Thus, $\hat{P} = VU^\top$ yields the conclusion. \square

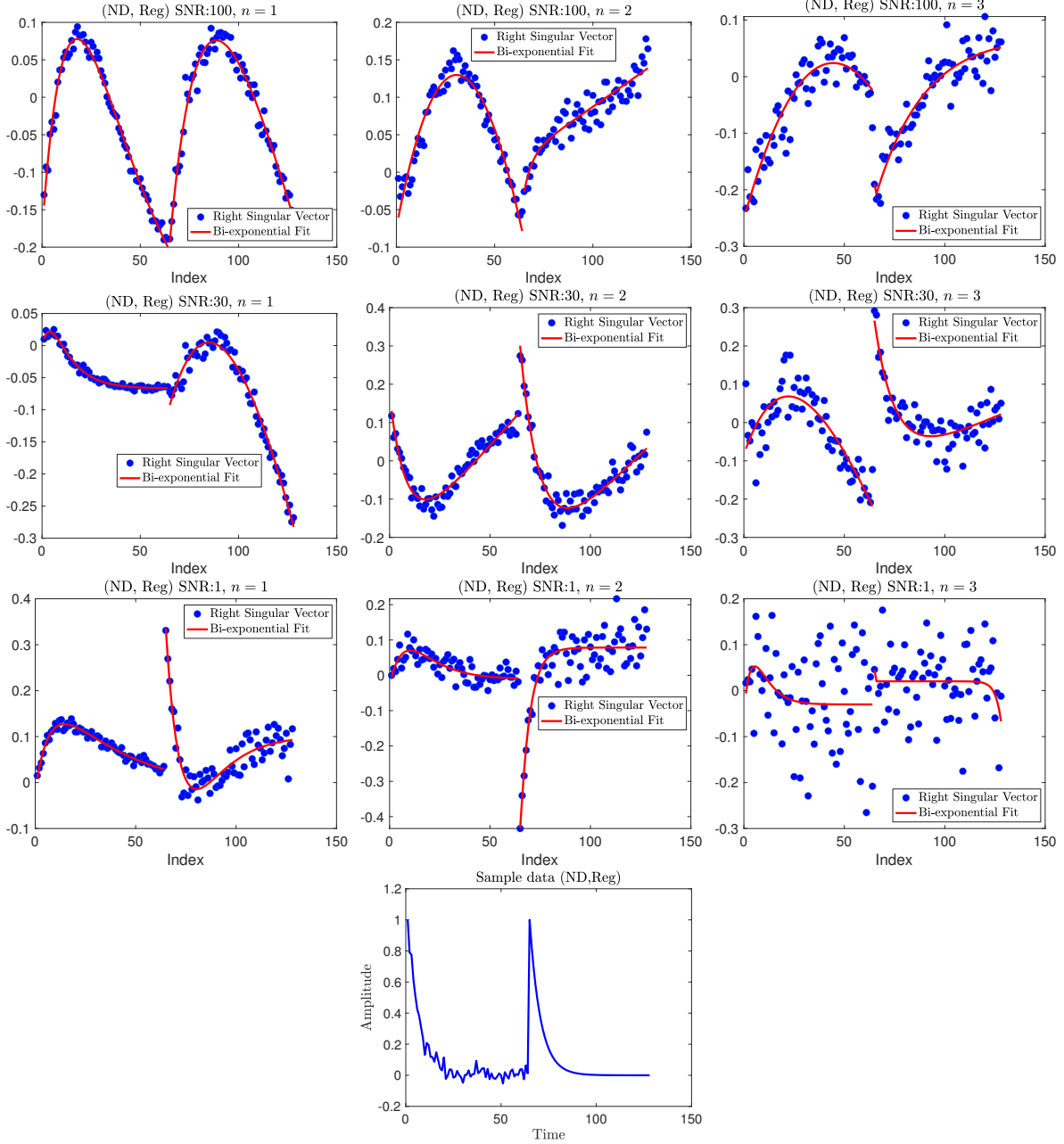


FIGURE 6. Here we visualize the first three right singular vectors of (ND, Reg) neural networks trained on the concatenation of noisy and NLLS-regularized smooth signals (shown below the center column) from a decaying biexponential model. Top to bottom: σ , corresponding to SNR values of 1, 30, 100, left to right: n th right singular vector of W_1 for $n = 1, 2, 3$. Each panel corresponds to a particular combination of SNR and n th singular vector. We demonstrate that these singular vectors can be fit with biexponential curves (red). The singular vectors exhibit breaks between the 64th and 65th samples, mimicking the structure of the input training data. As shown, a different biexponential curve is learned for each half. The curves learned for the initial, noisy, half of the SV's is markedly different from the curves learned for the second, smooth, half, enabling us to better understand the manner in which (ND,Reg) generalizes better than (ND,ND). Interestingly, the leading singular vectors for low SNR are highly noisy and fail to fit the biexponential model as n (the index of the singular vector) increases.

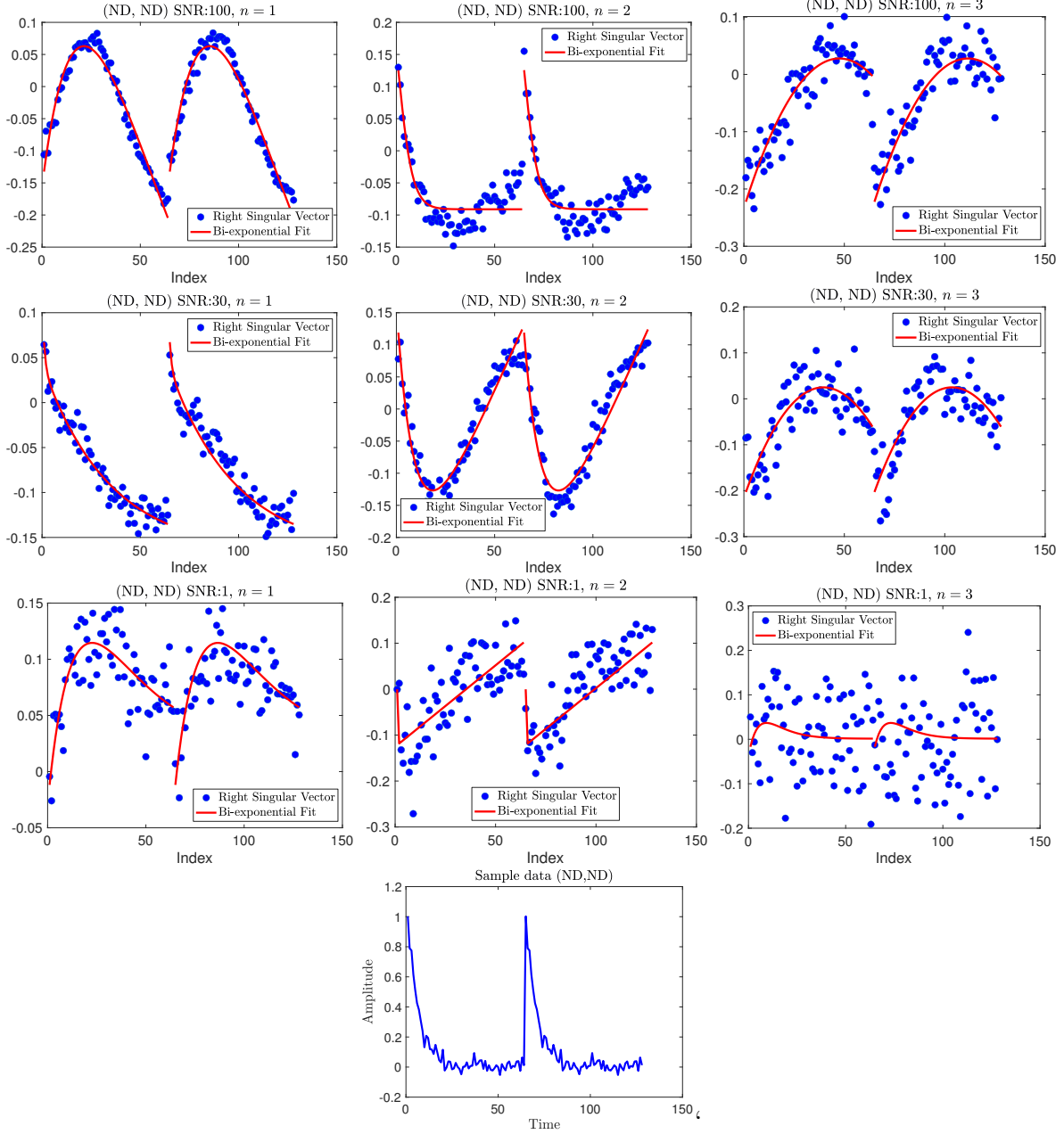


FIGURE 7. Here we visualize the right singular vector of (ND, ND) neural networks trained on concatenation of the same noisy signal (last row central panel) from a decaying biexponential model. Top to bottom: $\sigma^{-1} = 1, 30, 100$, left to right: n th right singular vector of W_1 for $n = 1, 2, 3$. We observe a similar pattern to the (ND, Reg) networks where the singular vectors can be fit with a biexponential model, concluding that singular vector model learning is truly a consequence of the data and not the concatenation procedure. Clearly, since both halves of the data are the same, the singular vectors on both halves the data are also nearly identical. Thus the signal model library learned by the weights of the NN is less diverse, and may be responsible for the lower test accuracy of the NN. Note that the drop in quality of singular vector approximation for low SNR is even more pronounced for the (ND,ND) case.

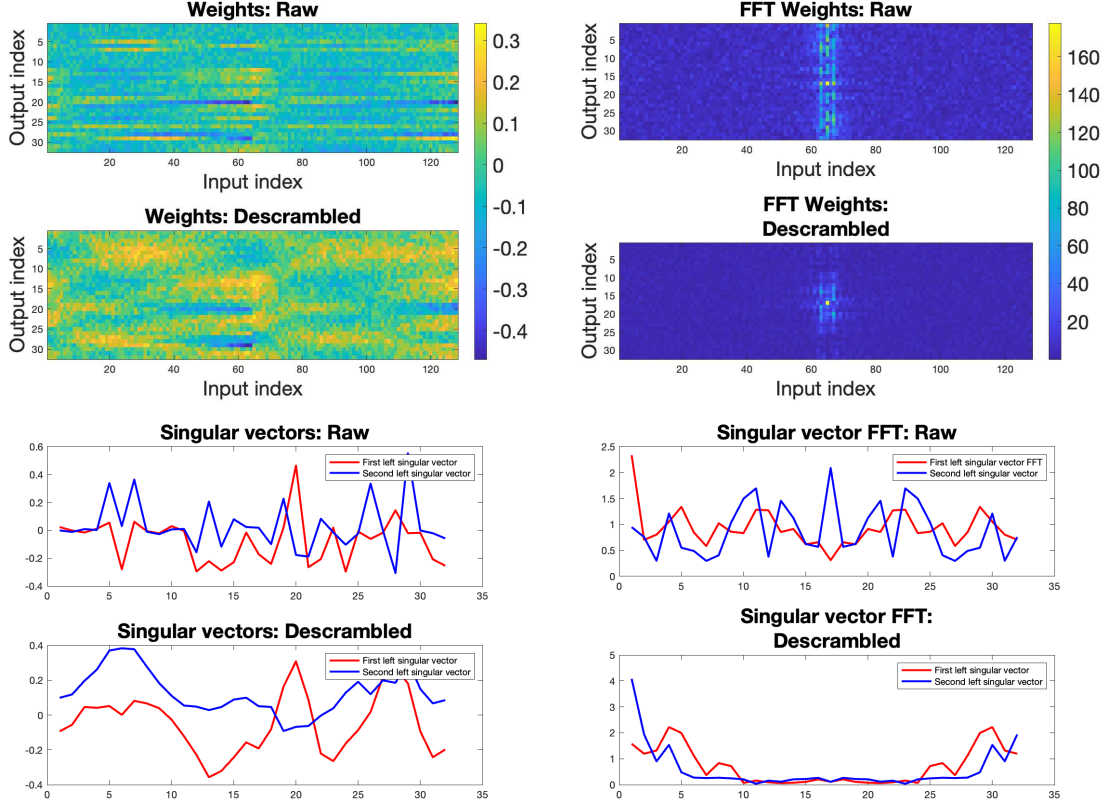


FIGURE 8. Effect of descrambling the first layer of an (ND, Reg) network with input data of SNR 10. However, the interpretation of this descrambled system is more elusive than that for the unscrambled DEERNet, with no clear pattern emerging from its Fourier signature or from the descrambled singular vectors. In fact, after descrambling with noise-only data, we found the descrambled matrices much more interpretable. The reason for this is clarified by Theorem 1, which indicates that the result of this process was to visualize the right singular vectors, which can be identified with samples of a biexponential model.

REFERENCES

- [1] Jake L Amey, Jake Keeley, Tajwar Choudhury, and Ilya Kuprov. “Neural network interpretation using descrambler groups”. In: *Proceedings of the National Academy of Sciences* 118.5 (2021).
- [2] Andrew M Saxe, James L McClelland, and Surya Ganguli. “A mathematical theory of semantic development in deep neural networks”. In: *Proceedings of the National Academy of Sciences* 116.23 (2019), pp. 11537–11546.
- [3] Erik Strumbelj and Igor Kononenko. “An efficient explanation of individual classifications using game theory”. In: *The Journal of Machine Learning Research* 11 (2010), pp. 1–18.
- [4] Feng Wang, Haijun Liu, and Jian Cheng. “Visualizing deep neural network by alternately image blurring and deblurring”. In: *Neural Networks* 97 (2018), pp. 162–172.
- [5] Aravindh Mahendran and Andrea Vedaldi. “Understanding deep image representations by inverting them”. In: *Proceedings of the IEEE conference on computer vision and pattern recognition*. 2015, pp. 5188–5196.
- [6] Anh Nguyen, Alexey Dosovitskiy, Jason Yosinski, Thomas Brox, and Jeff Clune. “Synthesizing the preferred inputs for neurons in neural networks via deep generator networks”. In: *Advances in neural information processing systems* 29 (2016).
- [7] Fahim Dalvi, Nadir Durrani, Hassan Sajjad, Yonatan Belinkov, Anthony Bau, and James Glass. “What is one grain of sand in the desert? analyzing individual neurons in deep nlp models”. In: *Proceedings of the AAAI Conference on Artificial Intelligence*. Vol. 33. 01. 2019, pp. 6309–6317.
- [8] Dumitru Erhan, Yoshua Bengio, Aaron Courville, and Pascal Vincent. “Visualizing higher-layer features of a deep network”. In: *University of Montreal* 1341.3 (2009), p. 1.
- [9] Anh Nguyen, Jeff Clune, Yoshua Bengio, Alexey Dosovitskiy, and Jason Yosinski. “Plug & play generative networks: Conditional iterative generation of images in latent space”. In: *Proceedings of the IEEE conference on computer vision and pattern recognition*. 2017, pp. 4467–4477.
- [10] Karen Simonyan, Andrea Vedaldi, and Andrew Zisserman. “Deep inside convolutional networks: Visualising image classification models and saliency maps”. In: *arXiv preprint arXiv:1312.6034* (2013).
- [11] Maithra Raghu, Justin Gilmer, Jason Yosinski, and Jascha Sohl-Dickstein. “Svcca: Singular vector canonical correlation analysis for deep learning dynamics and interpretability”. In: *Advances in neural information processing systems* 30 (2017).
- [12] Charles Godfrey, Davis Brown, Tegan Emerson, and Henry Kvinge. “On the Symmetries of Deep Learning Models and their Internal Representations”. In: *arXiv preprint arXiv:2205.14258* (2022).
- [13] Brenda Praggastis, Davis Brown, Carlos Ortiz Marrero, Emilie Purvine, Madelyn Shapiro, and Bei Wang. “The SVD of Convolutional Weights: A CNN Interpretability Framework”. In: *arXiv preprint arXiv:2208.06894* (2022).
- [14] Sven Hammarling. “The singular value decomposition in multivariate statistics”. In: *ACM Signum Newsletter* 20.3 (1985), pp. 2–25.
- [15] Erkki Oja. “The nonlinear PCA learning rule in independent component analysis”. In: *Neurocomputing* 17.1 (1997), pp. 25–45.

- [16] Michael E Wall, Andreas Rechtsteiner, and Luis M Rocha. “Singular value decomposition and principal component analysis”. In: *A practical approach to microarray data analysis*. Springer, 2003, pp. 91–109.
- [17] Isaac J Schoenberg. “Metric spaces and positive definite functions”. In: *Transactions of the American Mathematical Society* 44.3 (1938), pp. 522–536.
- [18] Benyamin Ghojogh, Ali Ghodsi, Fakhri Karay, and Mark Crowley. “Multidimensional scaling, sammon mapping, and isomap: Tutorial and survey”. In: *arXiv preprint arXiv:2009.08136* (2020).
- [19] J Álvarez-Vizoso, Robert Arn, Michael Kirby, Chris Peterson, and Bruce Draper. “Geometry of curves in R^n from the local singular value decomposition”. In: *Linear Algebra and its Applications* 571 (2019), pp. 180–202.
- [20] Robert T Arn, Pradyumna Narayana, Tegan Emerson, Bruce A Draper, Michael Kirby, and Chris Peterson. “Motion segmentation via generalized curvatures”. In: *IEEE transactions on pattern analysis and machine intelligence* 41.12 (2018), pp. 2919–2932.
- [21] Gao Daqi and Wu Shouyi. “An optimization method for the topological structures of feed-forward multi-layer neural networks”. In: *Pattern recognition* 31.9 (1998), pp. 1337–1342.
- [22] C-S Cheng. “A neural network approach for the analysis of control chart patterns”. In: *International Journal of Production Research* 35.3 (1997), pp. 667–697.
- [23] Huanrui Yang, Minxue Tang, Wei Wen, Feng Yan, Daniel Hu, Ang Li, Hai Li, and Yiran Chen. “Learning low-rank deep neural networks via singular vector orthogonality regularization and singular value sparsification”. In: *Proceedings of the IEEE/CVF conference on computer vision and pattern recognition workshops*. 2020, pp. 678–679.
- [24] Shengze Cai, Zhiping Mao, Zhicheng Wang, Minglang Yin, and George Em Karniadakis. “Physics-informed neural networks (PINNs) for fluid mechanics: A review”. In: *Acta Mechanica Sinica* (2022), pp. 1–12.
- [25] Alice Lucas, Michael Iliadis, Rafael Molina, and Aggelos K Katsaggelos. “Using deep neural networks for inverse problems in imaging: beyond analytical methods”. In: *IEEE Signal Processing Magazine* 35.1 (2018), pp. 20–36.
- [26] Jonas Adler and Ozan Öktem. “Solving ill-posed inverse problems using iterative deep neural networks”. In: *Inverse Problems* 33.12 (2017), p. 124007.
- [27] Tatiana A Bubba, Mathilde Galinier, Matti Lassas, Marco Prato, Luca Ratti, and Samuli Siltanen. “Deep neural networks for inverse problems with pseudodifferential operators: An application to limited-angle tomography”. In: *SIAM* (2021).
- [28] Steven G Worswick, James A Spencer, Gunnar Jeschke, and Ilya Kuprov. “Deep neural network processing of DEER data”. In: *Science advances* 4.8 (2018), eaat5218.
- [29] Vitaly Feldman and Chiyuan Zhang. “What neural networks memorize and why: Discovering the long tail via influence estimation”. In: *Advances in Neural Information Processing Systems* 33 (2020), pp. 2881–2891.
- [30] Peter D. Lax. *Linear Algebra and Its Applications*. Second. Hoboken, NJ: Wiley-Interscience, 2007. ISBN: 9780471751564 0471751561.
- [31] Lloyd N Trefethen. *Spectral methods in MATLAB*. SIAM, 2000.
- [32] Michael Rozowski, Jonathan Palumbo, Jay Bisen, Chuan Bi, Mustapha Bouhrara, Wojciech Czaja, and Richard G Spencer. “Input layer regularization for magnetic resonance relaxometry biexponential parameter estimation”. In: *Magnetic Resonance in Chemistry* 60.11. Special issue rapid communication. (2022), pp. 1076–1086.

- [33] Hau-Tieng Wu, Shu-Shua Hseu, Mauo-Ying Bien, Yu Ru Kou, and Ingrid Daubechies. “Evaluating physiological dynamics via synchrosqueezing: Prediction of ventilator weaning”. In: *IEEE Transactions on Biomedical Engineering* 61.3 (2013), pp. 736–744.
- [34] Hau-Tieng Wu, Yi-Hsin Chan, Yu-Ting Lin, and Yung-Hsin Yeh. “Using synchrosqueezing transform to discover breathing dynamics from ECG signals”. In: *Applied and Computational Harmonic Analysis* 36.2 (2014), pp. 354–359.
- [35] Roberto H Herrera, Jiajun Han, and Mirko van der Baan. “Applications of the synchrosqueezing transform in seismic time-frequency analysis”. In: *Geophysics* 79.3 (2014), pp. V55–V64.
- [36] Jean Baptiste Tary, Roberto Henry Herrera, Jiajun Han, and Mirko van der Baan. “Spectral estimation—What is new? What is next?”. In: *Reviews of Geophysics* 52.4 (2014), pp. 723–749.
- [37] Haizhao Yang, Jianfeng Lu, and Lexing Ying. “Crystal image analysis using 2D synchrosqueezed transforms”. In: *Multiscale Modeling & Simulation* 13.4 (2015), pp. 1542–1572.
- [38] Haizhao Yang, Jianfeng Lu, William P Brown, Ingrid Daubechies, and Lexing Ying. “Quantitative canvas weave analysis using 2-D synchrosqueezed transforms: Application of time-frequency analysis to art investigation”. In: *IEEE Signal Processing Magazine* 32.4 (2015), pp. 55–63.
- [39] Jianfeng Lu, Benedikt Wirth, and Haizhao Yang. “Combining 2D synchrosqueezed wave packet transform with optimization for crystal image analysis”. In: *Journal of the Mechanics and Physics of Solids* 89 (2016), pp. 194–210.
- [40] Haizhao Yang. “Synchrosqueezed wave packet transforms and diffeomorphism based spectral analysis for 1D general mode decompositions”. In: *Applied and Computational Harmonic Analysis* 39.1 (2015), pp. 33–66.
- [41] Rok Cestnik and Markus Abel. “Inferring the dynamics of oscillatory systems using recurrent neural networks”. In: *Chaos: An Interdisciplinary Journal of Nonlinear Science* 29.6 (2019), p. 063128.
- [42] Andrew M Saxe, James L McClelland, and Surya Ganguli. “Exact solutions to the nonlinear dynamics of learning in deep linear neural networks”. In: *arXiv preprint arXiv:1312.6120* (2013).
- [43] Sergey Ioffe and Christian Szegedy. “Batch Normalization: Accelerating Deep Network Training by Reducing Internal Covariate Shift”. In: *Proceedings of the 32nd International Conference on Machine Learning*. Ed. by Francis Bach and David Blei. Vol. 37. Proceedings of Machine Learning Research. Lille, France: PMLR, July 2015, pp. 448–456. URL: <https://proceedings.mlr.press/v37/ioffe15.html>.
- [44] Simon Wiesler and Hermann Ney. “A Convergence Analysis of Log-Linear Training”. In: *Advances in Neural Information Processing Systems*. Ed. by J. Shawe-Taylor, R. Zemel, P. Bartlett, F. Pereira, and K.Q. Weinberger. Vol. 24. Curran Associates, Inc., 2011. URL: https://proceedings.neurips.cc/paper_files/paper/2011/file/e836d813fd184325132fca8edcdfb40e-Paper.pdf.
- [45] Hyvärinen Aapo, Hurri Jarmo, and O. Hoyer Patrick. *Natural Image Statistics: A Probabilistic Approach to Early Computational Vision*. Springer Publishing Company, 2009.
- [46] Richard G. Spencer and Chuan Bi. “A Tutorial Introduction to Inverse Problems in Magnetic Resonance”. In: *NMR in Biomedicine* 33.12 (2020). e4315 nbm.4315, e4315.

- DOI: <https://doi.org/10.1002/nbm.4315>. eprint: <https://analyticalsciencejournals.onlinelibrary.wiley.com/doi/pdf/10.1002/nbm.4315>. URL: <https://analyticalsciencejournals.onlinelibrary.wiley.com/doi/abs/10.1002/nbm.4315>.
- [47] David A Reiter, Ping-Chang Lin, Kenneth W Fishbein, and Richard G Spencer. “Multicomponent T2 relaxation analysis in cartilage”. In: *Magnetic Resonance in Medicine: An Official Journal of the International Society for Magnetic Resonance in Medicine* 61.4 (2009), pp. 803–809.
 - [48] David A Reiter, Remigio A Roque, Ping-Chang Lin, Onyi Irrechukwu, Stephen Doty, Dan L Longo, Nancy Pleshko, and Richard G Spencer. “Mapping proteoglycan-bound water in cartilage: improved specificity of matrix assessment using multiexponential transverse relaxation analysis”. In: *Magnetic Resonance in Medicine* 65.2 (2011), pp. 377–384.
 - [49] Mustapha Bouhrara, David A Reiter, and Richard G Spencer. “Bayesian analysis of transverse signal decay with application to human brain”. In: *Magnetic resonance in medicine* 74.3 (2015), pp. 785–802.
 - [50] Mustapha Bouhrara, David A Reiter, Hasan Celik, Jean-Marie Bonny, Vanessa Lukas, Kenneth W Fishbein, and Richard G Spencer. “Incorporation of Rician noise in the analysis of biexponential transverse relaxation in cartilage using a multiple gradient echo sequence at 3 and 7 Tesla”. In: *Magnetic resonance in medicine* 73.1 (2015), pp. 352–366.
 - [51] Mustapha Bouhrara, David A Reiter, Kyle W Sexton, Christopher M Bergeron, Linda M Zukley, and Richard G Spencer. “Clinical high-resolution mapping of the proteoglycan-bound water fraction in articular cartilage of the human knee joint”. In: *Magnetic resonance imaging* 43 (2017), pp. 1–5.
 - [52] Richard G Spencer and Chuan Bi. “A tutorial introduction to inverse problems in magnetic resonance”. In: *NMR in Biomedicine* 33.12 (2020), e4315.
 - [53] Chuan Bi, Kenneth Fishbein, Mustapha Bouhrara, and Richard G Spencer. “Stabilization of parameter estimates from multiexponential decay through extension into higher dimensions”. In: *Scientific reports* 12.1 (2022), pp. 1–16.
 - [54] Richard Spencer, Ryan Neff, Chuan Bi, Radu Balan, and Zezheng Song. “Breaking the CRLB Barrier: Decreasing Mean Squared Error in Parameter Estimation Through Introduction of Regularization Bias”. In: *Bulletin of the American Physical Society* (2022).
 - [55] Zhaodi Zhang, Yiting Wu, Si Liu, Jing Liu, and Min Zhang. “Provably tightest linear approximation for robustness verification of sigmoid-like neural networks”. In: *arXiv preprint arXiv:2208.09872* (2022).
 - [56] Nasim Rahaman, Aristide Baratin, Devansh Arpit, Felix Draxler, Min Lin, Fred Hamprecht, Yoshua Bengio, and Aaron Courville. “On the spectral bias of neural networks”. In: *International Conference on Machine Learning*. PMLR. 2019, pp. 5301–5310.
 - [57] Nikunj Saunshi, Arushi Gupta, Mark Braverman, and Sanjeev Arora. “Understanding Influence Functions and Datamodels via Harmonic Analysis”. In: *arXiv preprint arXiv:2210.01072* (2022).
 - [58] Maithra Raghu, Ben Poole, Jon Kleinberg, Surya Ganguli, and Jascha Sohl-Dickstein. “On the expressive power of deep neural networks”. In: *international conference on machine learning*. PMLR. 2017, pp. 2847–2854.

- [59] Y. Yu, T. Wang, and R. J. Samworth. “A useful variant of the Davis–Kahan theorem for statisticians”. In: *Biometrika* 102.2 (Apr. 2014), pp. 315–323. ISSN: 0006-3444. DOI: [10.1093/biomet/asv008](https://doi.org/10.1093/biomet/asv008). eprint: <https://academic.oup.com/biomet/article-pdf/102/2/315/9642505/asv008.pdf>. URL: <https://doi.org/10.1093/biomet/asv008>.

DEPARTMENT OF MATHEMATICS, UNIVERSITY OF MARYLAND, COLLEGE PARK

NATIONAL INSTITUTE ON AGING, NATIONAL INSTITUTES OF HEALTH

DEPARTMENT OF MATHEMATICS, UNIVERSITY OF MARYLAND, COLLEGE PARK